Gain-saturation-induced self-sustained oscillations in non-Hermitian optomechanics

X. Z. Hao,[1] X. Y. Zhang,[1,*] Y. H. Zhou,[2] Wenlin Li,[3] S. C. Hou,[1] and X. X. Yi[4,†]

[1]*Department of Physics, Dalian Maritime University, Dalian 116026, China*

[2]*Quantum Information Research Center, Shangrao Normal University, Shangrao 334000, China*

[3]*School of Science and Technology, Physics Division, University of Camerino, I-62032 Camerino (MC), Italy*

[4]*Center for Quantum Sciences and School of Physics, Northeast Normal University, Changchun 130024, China*

(Received 16 March 2021; accepted 28 April 2021; published 12 May 2021)

We explore the classical dynamics of a non-Hermitian compound optomechanical system. By resorting to the method used in laser theory, we derived the classical dynamical equations of the system which incorporate the gain saturation effect of the gain medium. By simulating the classical evolutions of the system, we find that as long as the initial state of the cavities is not in the vacuum state the gain medium will amplify the light energy stored initially in the system and drive the mechanical oscillator into self-sustained oscillation although there is no extra optical drive for the system. Self-sustained oscillation can be formed in both the nonlinear *PT* symmetry and *PT* symmetry-broken phase. We also find that the oscillation amplitudes of the mechanical oscillator are more sensitive to the gain saturation of the gain medium than the gain coefficient. Multistability of the self-sustained oscillation also appears in our model. Our paper provides a deeper insight into the influence of non-Hermiticity on the dynamics of optomechanical systems and a tool for device applications.

DOI: 10.1103/PhysRevA.103.053508

I. INTRODUCTION

Non-Hermitian systems, the dynamics of which are described by non-Hermitian Hamiltonians, have attracted intense interest on both theoretical and experimental fronts in recent years. Among the various non-Hermitian systems, a class of non-Hermitian Hamiltonians that has triggered a surge of interest is parity-time (*PT*) symmetric systems the Hamiltonians of which commute with a *PT* operator [1]. A *PT* symmetric Hamiltonian can exhibit two distinct phases: a *PT* symmetry phase, where the eigenvalues of the Hamiltonian are real despite its non-Hermiticity, and a *PT* symmetry-broken phase where the Hamiltonian supports complex conjugate pairs. At the transition, exceptional points, where both the eigenvalues and eigenvectors of the Hamiltonian coalescence, emerge [2,3]. Non-Hermitian quantum theory has been applied to a variety of subfields (for review, see Ref. [4]), including topological systems [5–17], optical systems [18–27], acoustics [28–31], electrical circuits [32–36], plasmonics [37], and metamaterials [38]. Non-Hermitian systems have many unique features that are either impossible or difficult to be implemented in their Hermitian counterparts, e.g., asymmetric mode conversion [39,40], loss-induced lasing [41,42], enhanced sensitivity of sensors near exceptional points [43,44] and non-Hermitian skin effect [5,45,46].

In optical realizations, the commonly used non-Hermitian structure consists of two coupled optical components, such as cavities or waveguides: one having loss and the other having gain which balances the loss of the other [20,22]. In these exotic structures with coupled gain and loss components, the interplay between gain and loss and the coupling strength between the two components can lead to entirely new features and device functionalities, such as power oscillations [18,20], single-mode *PT* lasers [47,48], unidirectional invisibility [49–51], and laser absorbers [52–54] to name a few. Recently, the concepts of *PT* symmetry have been extended to compound optomechanics (COM) [55–57], observing thresholdless phonon lasers [56], low-power chaos [57], multistability [58], etc. However, the above-mentioned researches on *PT* symmetric optical systems and COM have been investigated under the assumption that the gain and loss coefficients do not depend on the light intensity propagating in the systems. This assumption can lead to unphysical results, especially in the *PT* symmetry-broken phase, that the light intensity in the system will increase to infinity and the systems have no steady state [59–61]. Indeed, this assumption is only valid when the light intensity is so small that gain saturation effect, i.e., that the gain coefficient starts to decrease as the light intensity increases, does not come into play. When the light intensity increases to a large value, the optical gain is a function of light intensity and the gain saturation of the gain medium cannot be neglected. Based on this, a lot of researches have explored the influence of gain saturation on the dynamics of the *PT* symmetric optical systems [61–65], *PT* symmetric phonon lasers [66–68], and nonreciprocity [69–71]. It has been demonstrated that gain saturation can not only stabilize the *PT* symmetric optical systems, but also lead to *PT* symmetry restoration [61]. It has also been shown that gain saturation is responsible for light nonreciprocity in *PT* symmetric photonic systems [69].

In this paper, we investigate the influence of gain saturation on the dynamics of non-Hermitian COM, which has not been explored extensively. The system we considered contains an

*zhangxingyuan1@foxmail.com

†yixx@nenu.edu.cn

active cavity and a passive cavity to which the mechanical oscillator couples. In order to describe the dynamics of the system, we resort to the laser theory [72], i.e., the gain medium in the active cavity is modeled as inverted two-level atoms. In addition to the gain medium, we also put an ensemble of two-level atoms, which are in their ground states initially, in the passive cavity to induce photon loss. As the cavities couple to their surroundings inevitably in practice, we also considered a constant intrinsic photon decay rate for both the two cavities, which is ignored in the previous investigations of non-Hermitian COM. By adiabatically eliminating the gain and loss medium, we derived the classical dynamical equations of the non-Hermitian COM, which incorporate the gain and loss saturation effects of the gain and loss medium. By simulating the classical equations, we find that the gain saturation can play the role of optical drive and induce self-sustained oscillations (SSOs) of the mechanical oscillator although the system has no extra optical drive. The phenomenon that SSOs can be formed without external drive is due to the nonlinearity of the system. This phenomenon can also be found in the van der Pol oscillator the damping rate of which is nonlinear [73]. We also investigate the dependence of the oscillation amplitude of the mechanical oscillator on the gain coefficient and gain saturation of the gain medium. We also find that the intrinsic photon decay rates of the two cavities have a great influence on the dynamics of the system. The mechanical oscillator will settle into chaoslike motion if the intrinsic photon decay rates are neglected, whereas the mechanical oscillator settles into SSO even though the intrinsic photon decay rates are small values.

The paper is organized as follows. In Sec. II, we give the model that we considered in this paper. The classical dynamics of the system, including the gain-saturation-induced SSO, is investigated in Sec. III. In this section, we also study the influence of the gain coefficient and gain saturation on the oscillation amplitude of the mechanical oscillator. The influence of the intrinsic decay rates of the two cavities on the dynamics of the system is also investigated in this section. Finally, we summarize our results in Sec. IV.

II. THEORETICAL MODEL OF THE NON-HERMITIAN COM WITH GAIN AND LOSS SATURATION

The system we consider in this paper consists of two cavities and one mechanical oscillator (see Fig. 1). The mechanical oscillator couples to cavity 2, which is coupled to an ensemble of two-level atoms (loss medium). Cavity 1 couples to a gain medium which is modeled as an ensemble of inverted two-level atoms. It should be noted that in reality the gain medium is composed of multiple-level atoms, but it can be mapped to an effective two-level model provided that there is only one lasing transition [74]. The two cavities couple to each other through evanescent coupling which can be tuned by changing the distance between the two cavities. In order to investigate the classical dynamics of the non-Hermitian COM, we assume that the decay rates of the two-level atoms are much larger than the characteristic timescales of the optomechanical system. By adiabatically eliminating the two-level atoms, the classical dynamical equations of the non-Hermitian

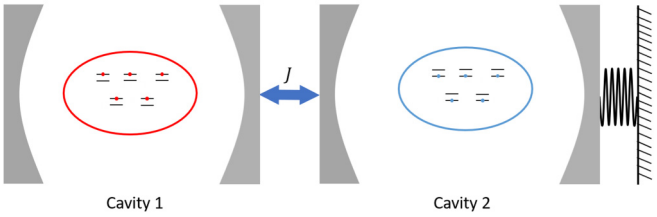

FIG. 1. Schematic diagram of the non-Hermitian COM. It includes a passive cavity (cavity 2) coupled to an active cavity (cavity 1) with intercavity coupling strength J. The mechanical oscillator couples to cavity 2 by radiation pressure. The gain medium in cavity 1 is modeled via inverted two-level atoms. However, the atoms in cavity 2, which provides the cavity with loss saturation, are normal two-level atoms in their ground states.

COM can be described as

$$\begin{aligned}
\dot{\alpha}_1 &= -\kappa\alpha_1 + \frac{g_0}{1+\frac{|\alpha_1|^2}{n_0}}\alpha_1 - iJ\alpha_2,\\
\dot{\alpha}_2 &= -\kappa\alpha_2 - \frac{f_0}{1+\frac{|\alpha_2|^2}{n_0}}\alpha_2 - iJ\alpha_1 + ig_m\alpha_2 x,\\
\ddot{x} &= -\omega_m^2 x + g_m\omega_m|\alpha_2|^2 - \gamma_m\dot{x}.
\end{aligned} \tag{1}$$

The derivation of Eq. (1) is given in the Appendix. α_j $(j = 1, 2)$ is the field amplitude of the jth cavity and x is the displacement of the mechanical oscillator with frequency ω_m. Here, we assume that the two cavities have the same intrinsic decay rate κ. γ_m is the decay rate of the mechanical oscillator. J and g_m are the evanescent coupling strength between the two cavities and the optomechanical coupling strength per single photon, respectively. g_0 and f_0 are the gain and loss coefficients of the gain and loss medium, respectively. n_0 is the gain and loss saturation of the gain and loss medium. The formulas of g_0, f_0, and n_0 are given in the Appendix. In order to make the role each parameter plays clear, it is convenient to work with dimensionless quantities. We rescale the variables t, x, α_1, and α_2 as $\tilde{t} = \omega_m t$, $\tilde{x} = g_m x/\omega_m$, and $\tilde{\alpha}_j = \alpha_j/\sqrt{n_0}$ $(j = 1, 2)$, so the coupled equations Eq. (1) are changed into

$$\begin{aligned}
\frac{d\tilde{\alpha}_1}{d\tilde{t}} &= -\tilde{\kappa}\tilde{\alpha}_1 + \frac{\tilde{g}_0}{1+|\tilde{\alpha}_1|^2}\tilde{\alpha}_1 - i\tilde{J}\tilde{\alpha}_2,\\
\frac{d\tilde{\alpha}_2}{d\tilde{t}} &= -\tilde{\kappa}\tilde{\alpha}_2 - \frac{\tilde{f}_0}{1+|\tilde{\alpha}_2|^2}\tilde{\alpha}_2 - i\tilde{J}\tilde{\alpha}_1 + i\tilde{\alpha}_2\tilde{x},\\
\frac{d^2\tilde{x}}{d\tilde{t}^2} &= -\tilde{x} + \mathcal{P}_d|\tilde{\alpha}_2|^2 - \tilde{\gamma}_m\frac{d\tilde{x}}{d\tilde{t}},
\end{aligned} \tag{2}$$

where the dimensionless parameters are

$$\begin{aligned}
&\tilde{\kappa} = \kappa/\omega_m, \quad \tilde{g}_0 = g_0/\omega_m, \quad \tilde{f}_0 = f_0/\omega_m,\\
&\tilde{J} = J/\omega_m, \quad \tilde{\gamma}_m = \gamma_m/\omega_m, \quad \mathcal{P}_d = \frac{g_m^2 n_0}{\omega_m^2}.
\end{aligned}$$

Compared with Eq. (2) in Ref. [75], we find that the saturation coefficient n_0 played the role of optical drive to drive the mechanical oscillator into SSO although there is no extra laser to drive the cavities.

In order to get the classical dynamics of the system, we simulate Eq. (2) numerically as the equations are too

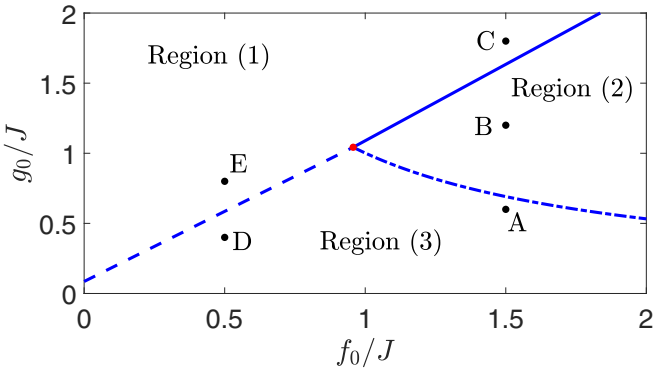

FIG. 2. Phase diagram of the *PT* symmetric dimer considered in Ref. [61] in the parameter space of g_0 and f_0. The parameter space is divided into three regions by three curves, i.e., $g_0 = (2\kappa + f_0)$ (dashed blue line), $g_0 = f_0(J+\kappa)/(J-\kappa)$ (solid blue line), and $g_0 = J^2/(\kappa + f_0) + \kappa$ (blue dot-dashed line). The three curves intersect at point $(J-\kappa, J+\kappa)$ (red dot). The time evolutions of the non-Hermitian COM for the parameters of the five black marked points, i.e., points A–E, will be shown below. The loss coefficient is $f_0 = 0.5J$ (point D and E) and $f_0 = 1.5J$ (point A–C). The gain coefficient is $g_0 = 0.6J$ (point A), $g_0 = 1.2J$ (point B), $g_0 = 1.8J$ (point C), $g_0 = 0.4J$ (point D), and $g_0 = 0.8J$ (point E).

complicated to solve analytically. To make the following results within experimental realizations, we simulate Eq. (2) by the parameters of the system which are accessible experimentally. These parameters are [22,56–58,76] $\omega_{c_1} = \omega_{c_2} = 2\pi \times 193$ THz, $\omega_m = 2\pi \times 23.4$ MHz, $\kappa = 3.14$ MHz, $\gamma_m = 0.24$ MHz, and $g_m = 2\pi \times 3.4$ KHz.

By setting $g_m = 0$, our model reduces to the model considered in Ref. [61]. In Ref. [61], the authors find that in the presence of nonlinear saturation effect the *PT* symmetric dimer has three different phases in the parameter space of g_0 and f_0 (see Fig. 2). In region 1, the two cavities exhibit limit cycles with the same field amplitude. The authors call this region the nonlinear *PT* symmetry phase as the nonlinear system has two real eigenvalues. In region 2, which is the nonlinear *PT* symmetry-broken phase, due to the saturation effects of the gain and loss medium the two cavities can have stationary solutions, but with different field amplitudes. The field amplitude in the active cavity is always larger than that in the passive cavity. Region 3 is a decay phase in which the field amplitudes in the two cavities always decay to zero no matter what the initial state of the system is. The reason is that in this region the gain rate is so small that it cannot compensate the total loss of the system. In Fig. 2, we have picked five points in the three regions, i.e., points A–E. In the following, we will simulate the time evolutions of the non-Hermitian COM for the parameters of the five points, respectively.

III. GAIN-SATURATION-INDUCED SSO

From Eq. (2), it is easy to see that $\tilde{\alpha}_1(t) = \tilde{\alpha}_2(t) = \tilde{x}(t) = 0$ is always a trivial steady-state solution of the system. However, this solution is unstable and the system will evolve into other solutions if the initial value of $\tilde{\alpha}_1$ or $\tilde{\alpha}_2$ deviates from zero slightly. So the initial values of $\tilde{\alpha}_1$ and $\tilde{\alpha}_2$ cannot all be zero to get nontrivial dynamics of the system. The initial nonzero value of $\tilde{\alpha}_1$ or $\tilde{\alpha}_2$ means that at least one of the two cavities is not in vacuum initially. For simplification, we assume that initially the two cavities are in coherent states with random field amplitudes, i.e., $\tilde{\alpha}_1(0) = \alpha_1(0)/\sqrt{n_0}$ and $\tilde{\alpha}_2(0) = \alpha_2(0)/\sqrt{n_0}$ where $\alpha_1(0)$ and $\alpha_2(0)$ are the initial field amplitudes of cavity 1 and 2, respectively. The values of $\alpha_1(0)$ and $\alpha_2(0)$ are random complex numbers, satisfying $|\alpha_j(0)| \in (0, 1)$ $(j = 1, 2)$. For the mechanical oscillator, we assume $x(0) = \dot{x}(0) = 0$ throughout the paper.

Figure 3 shows the periodic solutions achieved by the system at long enough time for the parameters of point B, C, and E in Fig. 2, with initial values $\alpha_1(0) = \alpha_2(0) = 0.5$. Time evolutions of the system for the parameters of point A and D are not shown, as in the decay phase the two cavities always decay into vacuum and cannot influence the mechanical oscillator. Figures 3(a)–3(c) clearly show that the position of the mechanical oscillator exhibits sinusoidal oscillation when time is long enough. Figures 3(a) and 3(d) and Figs. 3(b) and 3(e) show the time evolutions of the system for the parameters of point C and E, respectively. From these figures, we can see that the classical dynamics of the system are similar for the parameters of point C and E, except that the mechanical oscillator achieves self-sustained oscillation faster at point C than at point E. This is because at point C the system has larger gain coefficient and the field amplitude increases quickly. The similarity of the classical dynamics for point C and E is due to the fact that both the two points are in the nonlinear *PT* symmetry phase and the physical formalism can be understood as follows. The two cavity modes form two supermodes $\hat{a}_\pm = (\hat{a}_1 \pm e^{\pm i\theta}\hat{a}_2)/\sqrt{2}$ with $\sin(\theta) = \kappa(g_0 + f_0)/[J(g_0 - f_0)]$. The nonlinear eigenvalues of the two supermodes are $\lambda_\pm = \pm J\sqrt{1 - \sin^2(\theta)}$ [61]. When transforming into the representation of the two supermodes, the optomechanical coupling $\hat{a}_2^\dagger \hat{a}_2 \hat{x}$ can be written as

$$\hat{a}_2^\dagger \hat{a}_2 \hat{x} = \tfrac{1}{2}(\hat{a}_+^\dagger \hat{a}_+ + \hat{a}_-^\dagger \hat{a}_-)\hat{x} - \tfrac{1}{2}(\hat{a}_+^\dagger \hat{a}_- + \hat{a}_+ \hat{a}_-^\dagger)\hat{x}. \quad (3)$$

The frequency difference of the two supermodes is $0.9827\omega_m$ and $0.8822\omega_m$ for the parameters of point E and C, respectively. So for both point C and E, the first term is large detuning and can be neglected. By keeping only the near resonant term, the interaction between the two supermodes and the mechanical oscillator has the form $\hat{a}_+^\dagger \hat{a}_- \hat{b} + \hat{a}_+ \hat{a}_-^\dagger \hat{b}$ and is the same interaction that is used to generate phonon lasing [56,77]. So the physical mechanism of SSO in the nonlinear *PT* symmetry phase is similar to that of phonon lasing. The optical inversion between the two supermodes continuously transmits energy to the mechanical oscillator through photon scattering. When the energy provided by the optical inversion per oscillation period is compensated by the energy loss induced by the mechanical environment, the mechanical oscillator settles into self-sustained oscillation.

In contrast to the classical dynamics of the system in the nonlinear *PT* symmetry phase, in the nonlinear *PT* symmetry-broken phase the oscillation amplitude of the mechanical oscillator experiences exponential increasing before the mechanical oscillator reaches self-sustained oscillation [see Fig. 3(c)]. One interesting phenomenon is that in the initial short time the evolution of the field intensities in the two cavities is the same as the situation without mechanical

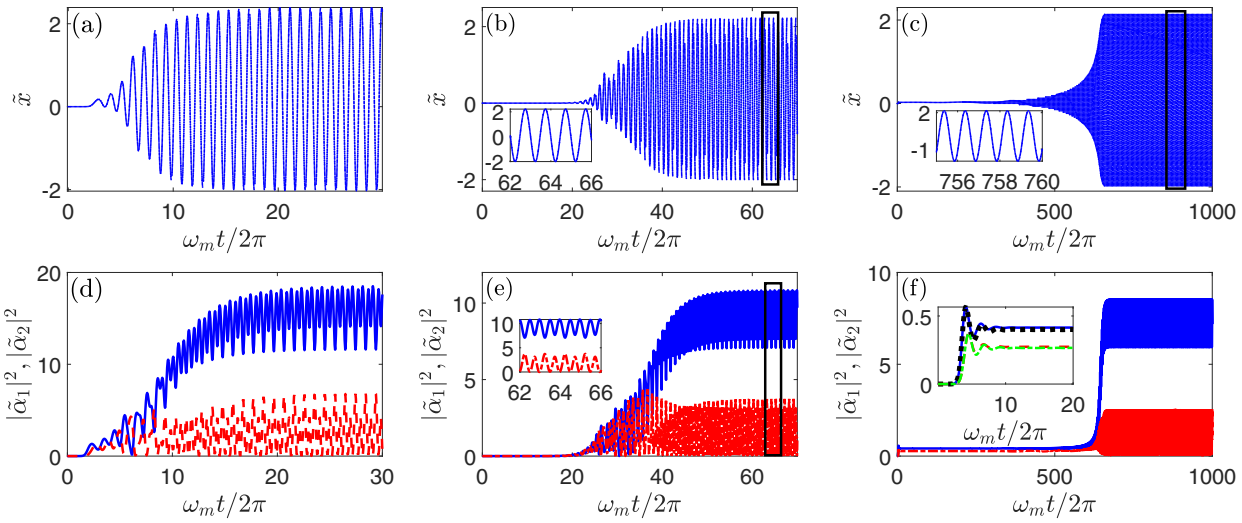

FIG. 3. (a)–(c) Time evolution of $\tilde{x}$ and (d)–(f) time evolution of the light energy stored in the active cavity $|\tilde{\alpha}_1|^2$ (blue solid line) and the passive cavity $|\tilde{\alpha}_2|^2$ (red dot-dashed line) for the parameters of point C (a), (d), point E (b), (e), and point B (c), (f) in Fig. 2. Insets in (b), (c), and (e) show the zoom of the area indicated by the black box. The inset in (f) shows the comparison for the evolutions of $|\tilde{\alpha}_1|^2$ and $|\tilde{\alpha}_2|^2$ in the initial short time with and without the optomechanical coupling. The blue solid line (red dashed line) and black dotted line (green dot-dashed line) give the dynamics of $|\tilde{\alpha}_1|^2$ ($|\tilde{\alpha}_2|^2$) with and without the optomechanical coupling, respectively. Other parameters are $J = 0.5\omega_m$ and $\mathcal{P}_d = 0.1$, which means that the gain and loss saturation is about $n_0 \approx 4.74\times10^6$.

oscillator [see the inset in Fig. 3(f)]. As the oscillation amplitude of the mechanical oscillator increases to a large value, the light intensities in the two cavities increase quickly. This means that the harmonic oscillations of the mechanical oscillator can enhance the amplification effect of the gain medium. As the two supermodes formed by the two cavities are degenerate in the nonlinear PT symmetry-broken phase, the phonon-mediated photon scattering interaction $\hat{a}_+^\dagger \hat{a}_- \hat{b} + \hat{a}_+ \hat{a}_-^\dagger \hat{b}$ is large detuning. This means that the physical mechanism for the formation of self-sustained oscillations is different from that in the nonlinear PT symmetry phase. Indeed, the reason for the formation of SSO in the nonlinear PT symmetry-broken phase is the same as that of single cavity optomechanics [75], i.e., due to the radiation pressure exerted by the passive cavity on the mechanical oscillator. Compared with the formation of SSO in single cavity optomechanics, our model does not need extra cavity pump to drive the mechanical oscillator into SSO. This means that SSO is a state of the non-Hermitian optomechanical system itself and is not generated by external control. Actually, the gain cavity plays the role to provide the passive cavity with sufficient light field to drive the mechanical oscillator into SSO. In the beginning, the mechanical oscillator is at rest and has no influence on the dynamics of the two cavities. So the cavity reaches the stationary state that the non-Hermitian dimer achieves, quickly. Once the passive cavity is filled with enough strong light field, the passive cavity can drive the mechanical oscillator to oscillate. As the oscillation of the mechanical oscillator can enhance the amplification effect of the gain medium, the oscillation of the mechanical oscillator can further enhance the field strength in the passive cavity which in turn enhances the oscillation amplitude of the mechanical oscillator. This positive mutual feedback will continue until the mechanical oscillator reaches the SSO.

In Fig. 4(a), we plot the oscillation amplitudes $\mathcal{A}$ of the mechanical oscillator, which are obtained by simulating Eq. (2) with a set of random initial conditions, as a function of gain saturation with the gain coefficient $g_0 = 1.8J$ (nonlinear PT symmetry phase) and $g_0 = 1.2J$ (nonlinear PT symmetry-broken phase). From this figure, we can see that for small gain saturation, e.g., $n_0 < 2.3\times10^4$, the mechanical oscillator cannot settle into SSO in both the nonlinear PT symmetry and PT symmetry-broken phase. This is because the gain saturation indicates the ability of the gain medium to amplify the initial photons in the cavity and the larger the gain saturation is the larger the initial photons in the cavity can be amplified. When the gain saturation is small, the amplified optical field strength in the cavities is not strong enough to drive the mechanical oscillator into SSO. In this case, the dynamics of the two cavities are the same as the situation without mechanical oscillator. For moderate gain saturation, e.g., $2.3\times10^4 < n_0 < 2.3\times10^5$, the mechanical oscillator can achieve SSO in the nonlinear PT symmetry phase and cannot reach SSO in the nonlinear PT symmetry-broken phase. The reason for this phenomenon is that in the nonlinear PT symmetry phase the optical field transfers energy to the mechanical oscillator via the phonon-laser-like interaction, which is more efficient than the radiation pressure interaction. So the optical field strength required to form SSO in the nonlinear PT symmetry phase is smaller than that in the nonlinear PT symmetry-broken phase. For large gain saturation, e.g., $n_0 > 2.3\times10^5$, SSO can be achieved in both the nonlinear PT symmetry and PT symmetry-broken phase. In both the two phases, the oscillation amplitude increases as the gain saturation increases.

It is well known that in single cavity optomechanics multiple stable harmonic solutions of the mechanical oscillator with different oscillation amplitudes can be found for the same parameter, i.e., multistability [75]. However, in Fig. 4(a)

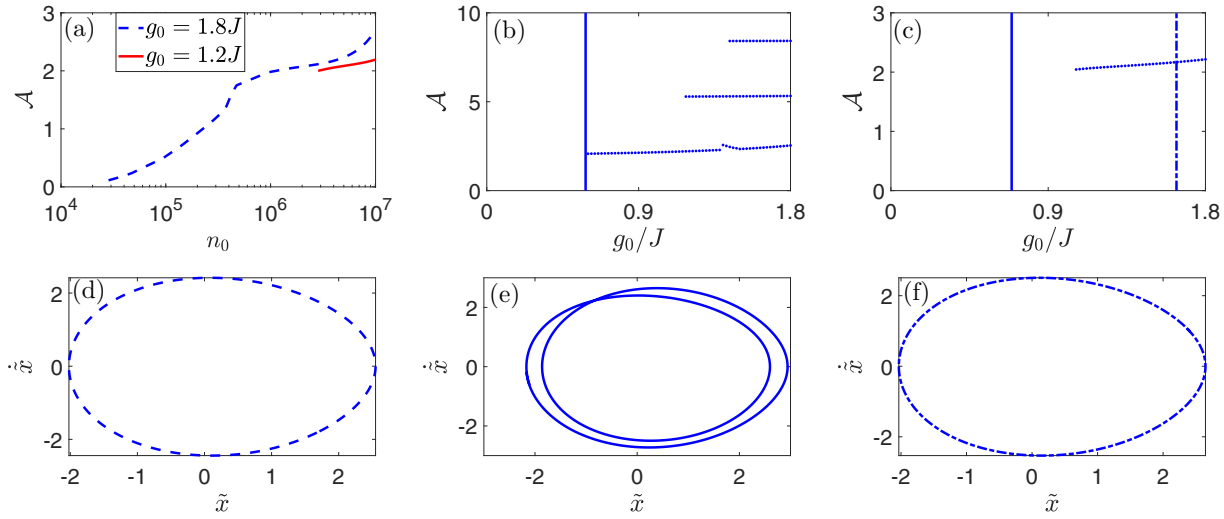

FIG. 4. (a) Oscillation amplitude $\mathcal{A}$ of the mechanical oscillator as a function of the gain saturation n_0 in the nonlinear PT symmetry phase ($g_0 = 1.8J$) and PT symmetry-broken phase ($g_0 = 1.2J$). The loss coefficient is $f_0 = 1.5J$. (b), (c) Oscillation amplitude $\mathcal{A}$ (blue dots) as a function of the gain coefficient with (b) $f_0 = 0.5J$ and (c) $f_0 = 1.5J$. The solid vertical line in (b) represents the boundary between the decay phase and the nonlinear PT symmetry phase. The left and right region of the solid vertical line are the decay phase and the nonlinear PT symmetry phase, respectively. The solid vertical line in (c) is the boundary between the decay phase and the nonlinear PT symmetry-broken phase and the vertical dot-dashed line is the boundary between the nonlinear PT symmetry-broken and PT symmetry phase. The oscillation amplitudes are obtained by simulating Eq. (2) with a set of random initial conditions. (d), (e) The trajectories of the mechanical oscillator in phase space for the branch of the smallest oscillation amplitude in (b). The gain coefficient is (d) $g_0 = 1.38J$, (e) $g_0 = 1.4J$, and (f) $g_0 = 1.5J$. The gain saturation in (b)–(f) is $n_0 \approx 4.74\times10^6$, i.e., $\mathcal{P}_d = 0.1$. Other parameters are the same as Fig. 3.

multistability does not show. This is because we restrict the initial values of $\tilde{\alpha}_1$ and $\tilde{\alpha}_2$ over a very small range of values, e.g., $\tilde{\alpha}_1(0) = \tilde{\alpha}_2(0) = 5\times10^{-4}$ with initial cavity field amplitude $\alpha_1 = \alpha_2 = 1$ and $n_0 = 4\times10^6$. If we enlarge the range of initial values for $\tilde{\alpha}_1$ and $\tilde{\alpha}_2$, e.g., $\tilde{\alpha}_j(0) \in (0, 10]$ $(j = 1, 2)$, the system can indeed exhibit multistability. However, large values of $\tilde{\alpha}_j(0)$ mean large initial cavity field amplitudes, e.g., $\alpha_1(0) = \alpha_2(0) = 10^4$ under the condition $\tilde{\alpha}_1(0) = \tilde{\alpha}_2(0) = 5$ and $n_0 = 4\times10^6$. Such large initial cavity field amplitudes are difficult to achieve in the PT symmetric dimer. So we do not consider such initial values of $\tilde{\alpha}_j(0)$. The small initial values of $\alpha_j(0) \in (0, 1)$ $(j = 1, 2)$ can be achieved by driving the two cavities with a very weak laser in a very short time. As both the driving time and the strength of the driving are small, the influence of the drive on the dynamics of the system can be neglected and the drive only alters the initial values of the cavity field amplitude. Another way to achieve small initial values of $\alpha_j(0)$ is to prepare the cavities on a coherent state before turning on the interaction between the cavities and the gain and loss medium. As the two cavities have intrinsic decay, the field amplitudes will experience exponential decrease and decay to zero as $t \to \infty$. If we turn on the interaction between the cavities and the gain and loss medium at finite time, the small initial values of $\alpha_j(0)$ can be achieved.

The oscillation amplitudes of the mechanical oscillator as a function of the gain coefficient are shown in Figs. 4(b) and 4(c) with $f_0 = 0.5J$ and $1.5J$, respectively. When $f_0 = 0.5J$, the system only has two phases, i.e., the decay phase and nonlinear PT symmetry phase. From Fig. 4(b), we can see that the mechanical oscillator cannot achieve SSO in the decay phase and can settle into SSO once the parameter enters the nonlinear PT symmetry phase. This is because in the decay phase both the cavities decay to vacuum as $t \to \infty$. In the nonlinear PT symmetry phase, the oscillation amplitude increases slowly as the gain coefficient increases and the system can exhibit multistability when g_0 increases to a large value. For the branch of the smallest oscillation amplitude in Fig. 4(b), there is an abrupt increase when $g_0 = 1.4J$. Then, the oscillation amplitude decreases until $g_0 = 1.5J$ after which the oscillation amplitude continues to increase as g_0 increases. Indeed, when $g_0 \in [1.4J, 1.5J)$ the mechanical oscillator settles into period-2 orbit instead of SSO [see the trajectory of the mechanical oscillator shown in Fig. 4(e) with $g_0 = 1.4J$]. In both the ranges of $g_0 < 1.4J$ and $g_0 \geqslant 1.5J$, the mechanical oscillator can achieve period-1 orbit, i.e., SSO [see the trajectories of the mechanical oscillator shown in Figs. 4(d) and 4(f) with $g_0 = 1.38J$ and $1.5J$, respectively]. For the other two branches of the oscillation amplitude shown in Figs. 4(b), the mechanical oscillator always settles into SSO. When $f_0 = 1.5J$, the system has three phases, i.e., the decay phase, nonlinear PT symmetry-broken phase, and PT symmetry phase. From Fig. 4(c), we can see that the system does not exhibit SSO in the decay phase. This is consistent with Fig. 4(b). In the nonlinear PT symmetry-broken phase, the system also does not exhibit SSO near the boundary of the decay phase and the nonlinear PT symmetry-broken phase. SSO is formed until the gain coefficient goes into the deep nonlinear PT symmetry-broken phase. This is because near the boundary between the decay phase and the nonlinear PT symmetry-broken phase the amplified optical field in the passive cavity is not strong enough to drive the mechanical oscillator into SSO. The amplified optical field in the passive cavity becomes larger as the gain coefficient increases. As the

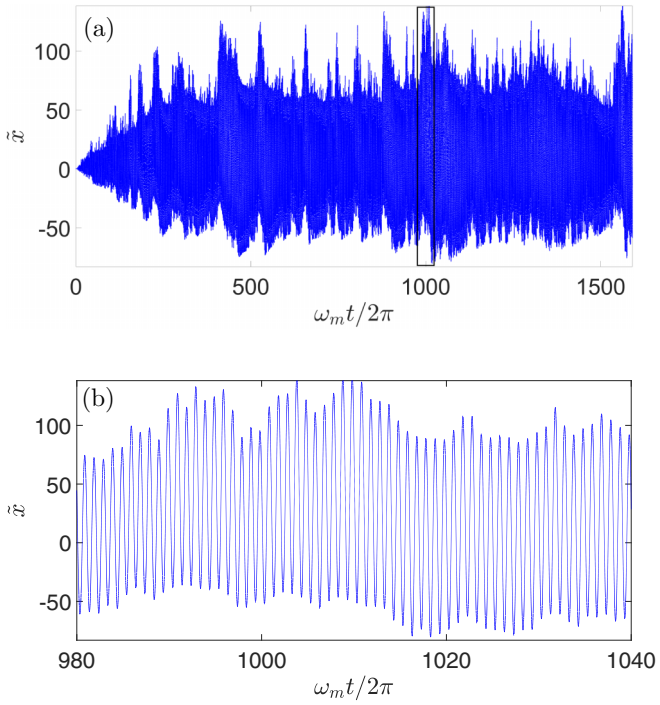

FIG. 5. (a) Dynamics of $\tilde{x}$ with $\kappa = 0$. Other parameters are the same as Fig. 3(a). (b) The zoom of the area indicated by the black box in (a).

gain coefficient goes deep into the nonlinear *PT* symmetry-broken phase, the optical field in the passive cavity will be amplified to a large value so that it can make the mechanical oscillator form SSO. In the nonlinear *PT* symmetry phase, the mechanical oscillator can always settle into SSO. Similar to Fig. 4(b), the oscillation amplitude also increases as the gain coefficient increases. Multistability also does not show in Fig. 4(c) and the reason is the same as that of Fig. 4(a). Comparing Figs. 4(b) and 4(c) with Fig. 4(a), we find that the oscillation amplitude of the mechanical oscillator is more sensitive to the change of gain saturation than the change of gain coefficient.

Before concluding this paper, we investigate the influence of the intrinsic decay of the two cavities on the classical dynamics of the system. In Fig. 5, we plot the dynamics of $\tilde{x}$ with $\kappa = 0$ for the parameters of point C in Fig. 2. The dynamics of $\tilde{x}$ with nonzero κ for the same parameters is shown in Fig. 3(a). From this figure, we can see that $\tilde{x}$ exhibits a chaoslike trajectory by setting $\kappa = 0$. However, by setting κ a small value, the dynamics of $\tilde{x}$ is SSO. This means that the intrinsic decay rates of the two cavities have a great influence on the dynamics of the system. In other words, the formation of SSO is resulted from the combined effect of the gain medium and the intrinsic decay of the cavities and SSO cannot be formed without either one of them. The gain medium provides energy to drive the mechanical oscillator and the intrinsic decay rate stabilizes the system. So the intrinsic decay rate κ, which is usually ignored in the previous researches of non-Hermitian optomechanical systems, cannot be ignored when studying the evolution of non-Hermitian optomechanical systems.

IV. CONCLUSION

We have investigated the influence of gain saturation on the classical dynamics of non-Hermitian COM. We find that if the initial cavity field amplitudes, which can be a very small value, are not zero, the mechanical oscillator can settle into SSO even if the system has no driving. This is because the gain medium can amplify the small optical field stored initially in the two cavities to a large optical field which can drive the mechanical oscillator into SSO. However, the physical mechanism for the formation of SSO is different in the nonlinear *PT* symmetry phase and nonlinear *PT* symmetry-broken phase. In the nonlinear *PT* symmetry phase, the two cavities form two nondegenerate optical supermodes and the mechanical oscillator settles into SSO due to the near resonant phonon-mediated photon scattering interaction, which is also used to generate phonon lasers, between the two optical supermodes and the mechanical oscillator. In the nonlinear *PT* symmetry-broken phase, the two optical supermodes formed by the two cavities are degenerate. This means that the phonon-mediated photon scattering interaction between the two optical supermodes and the mechanical oscillator is large detuned and cannot drive the mechanical oscillator into SSO. Indeed, in this case the reason for the formation of SSO is just due to the radiation pressure exerted by the passive cavity on the mechanical oscillator. In both the two phases, the oscillation amplitude of the mechanical oscillator increases as the gain coefficient and gain saturation increase. The oscillation amplitude is more sensitive to the increase of gain saturation than the gain coefficient. Our model can also exhibit multistability of SSO. We also find that the intrinsic decay rates of the two cavities, which are usually ignored in the previous investigations of non-Hermitian optomechanical systems, can have a great influence on the classical evolution of the system even though the decay rates are small. Our investigations provide a deeper insight into the classical dynamics of non-Hermitian optomechanical systems and a tool for manipulating phonons.

ACKNOWLEDGMENT

This work is supported by the National Natural Science Foundation of China under Grants No. 11775048 and No. 12005032.

APPENDIX

In the Appendix, we derive the classical dynamical equations of the non-Hermitian COM. Our starting point is the total Hamiltonian of the whole system which includes the two-level atoms of the gain and loss medium. The total Hamiltonian of the whole system is given by

$$\hat{H}_{\rm tot} = \sum_{j=1}^{2} \hbar\omega_{c_j} \hat{a}_j^\dagger \hat{a}_j + \hbar\omega_m \hat{b}^\dagger \hat{b} + \frac{\hbar\omega_a}{2} \sum_{j=1}^{2} \sum_{\mu=1}^{N} \hat{\sigma}_{j,\mu}^z + \sum_{j=1}^{2} \sum_{\mu=1}^{N} i\hbar g_j (\hat{a}_j^\dagger \hat{\sigma}_{j,\mu}^- - \hat{a}_j \hat{\sigma}_{j,\mu}^+) - \hbar g_m \hat{a}_2^\dagger \hat{a}_2 \hat{x} + \hbar J(\hat{a}_1^\dagger \hat{a}_2 + \hat{a}_2^\dagger \hat{a}_1). \tag{A1}$$

The terms in the first line of Eq. (A1) represent the free Hamilton of the system. $\hat{a}_j$ and $\hat{a}_j^\dagger$ $(j = 1, 2)$ are the annihilation and creation operators of the jth cavity with frequency ω_{c_j}. $\hat{b}$ is the annihilation operator of the mechanical oscillator with frequency ω_m. $\hat{\sigma}_{j,\mu}^z$ is the z-component Pauli operator for the μth atom in the jth cavity and N is the total number of atoms in each cavity. We have assumed that all the atoms in both cavities have the same level spacing ω_a. The first term in the second line represents the interaction between the atoms and the cavities. g_j is the coupling strength between the atoms and the cavity in the jth cavity and $\hat{\sigma}_{j,\mu}^+$ and $\hat{\sigma}_{j,\mu}^-$ are the ladder operators of the two-level atoms. The second term in the second line represents the radiation pressure exerted on the mechanical oscillator by cavity 2 and g_m is the optomechanical coupling strength per single photon. $\hat{x} = (\hat{b}^\dagger + \hat{b})/\sqrt{2}$ is the dimensionless displacement of the mechanical oscillator with respect to its equilibrium position. The last term represents the directional coupling between the two cavities with tunneling strength J. For simplicity, we assume that the atoms and the cavities are resonant, i.e., $\omega_{c_j} = \omega_a$. In the interaction picture with respect to $\hat{H}_0 = \sum_{j=1}^2 \hbar\omega_{c_j}\hat{a}_j^\dagger\hat{a}_j + \frac{\hbar\omega_a}{2}\sum_{j=1}^2\sum_{\mu=1}^N \hat{\sigma}_{j,\mu}^z$, the master equation of the system can be written as

$$\dot{\hat{\rho}} = -\frac{i}{\hbar}[\hat{H}_{\rm int}, \hat{\rho}] + \mathcal{L}_1\hat{\rho} + \mathcal{L}_2\hat{\rho} + \mathcal{L}_c\hat{\rho} + \mathcal{L}_m\hat{\rho}, \quad \text{(A2)}$$

where $\hat{\rho}$ is the reduced density matrix of the system and $\hat{H}_{\rm int}$ is

$$\hat{H}_{\rm int} = \hbar\omega_m\hat{b}^\dagger\hat{b} + \sum_{j=1}^2\sum_{\mu=1}^N i\hbar g_j(\hat{a}_j^\dagger\hat{\sigma}_{j,\mu}^- - \hat{a}_j\hat{\sigma}_{1,\mu}^+)$$
$$-\hbar g_m\hat{a}_2^\dagger\hat{a}_2\hat{x} + \hbar J(\hat{a}_1^\dagger\hat{a}_2 + \hat{a}_2^\dagger\hat{a}_1).$$

As we have modeled the gain medium in cavity 1 as inverted two-level atoms, so the dynamics of the gain medium can be equivalently described as two-level atoms coupled to an inverted oscillator heat bath which is introduced by Glauber [78]. So the dissipator of the atoms in cavity 1 can be written as [72]

$$\mathcal{L}_1\hat{\rho} = \sum_{\mu=1}^N\left(\frac{\gamma_1}{2}\bar{N}_1\mathcal{D}[\hat{\sigma}_{1,\mu}^-]\hat{\rho} + \frac{\gamma_1}{2}(\bar{N}_1+1)\mathcal{D}[\hat{\sigma}_{1,\mu}^+]\hat{\rho}\right),$$

with $\mathcal{D}[\hat{o}]\rho = 2\hat{o}\hat{\rho}\hat{o}^\dagger - \hat{o}^\dagger\hat{o}\hat{\rho} - \hat{\rho}\hat{o}^\dagger\hat{o}$. γ_1 is the damping rate of the atoms in cavity 1 and $\bar{N}_1$ is the average thermal photon number of the inverted oscillator heat bath. The third term in Eq. (A2) represents the dissipation process of the atoms in cavity 2, which can be written as

$$\mathcal{L}_2\hat{\rho} = \sum_{\mu=1}^N\left(\frac{\gamma_2}{2}(\bar{N}_2+1)\mathcal{D}[\hat{\sigma}_{2,\mu}^-]\hat{\rho} + \frac{\gamma_2}{2}\bar{N}_2\mathcal{D}[\hat{\sigma}_{2,\mu}^+]\hat{\rho}\right),$$

where γ_2 is the damping rate of the atoms in cavity 2 and $\bar{N}_2$ is the average thermal photon number of the reservoir that the atoms couple to. The fourth and fifth terms in Eq. (A2) represent the intrinsic dissipation of the cavities and the mechanical oscillator, respectively, which can be written as

$$\mathcal{L}_c\hat{\rho} = \kappa\mathcal{D}[\hat{a}_1]\hat{\rho} + \kappa\mathcal{D}[\hat{a}_2]\hat{\rho},$$
$$\mathcal{L}_m\hat{\rho} = \frac{\gamma_m}{2}\bar{N}_m\mathcal{D}[\hat{b}^\dagger]\hat{\rho} + \frac{\gamma_m}{2}(\bar{N}_m+1)\mathcal{D}[\hat{b}]\hat{\rho}.$$

Here, we have assumed that the intrinsic decay rates of the two cavities are the same, i.e., κ, and both the reservoirs of the two cavities are zero temperature. γ_m is the decay rate of the mechanical oscillator and $\bar{N}_m$ is the mean phonon number of the mechanical oscillator in equilibrium.

In the following, we will derive an effective equation of motion for the optomechanical system by adiabatically eliminating the two-level atoms. The adiabatic elimination will strictly be valid under the condition that decay rates of the two-level atoms in the two cavities are much larger than other characteristic timescales of the optomechanical system, i.e., $\gamma_1, \gamma_2 \gg \omega_m, \kappa, \gamma_m, g_m$. From now on, we assume that the condition of adiabatic elimination is fulfilled in our system. We use the projection operator techniques in phase space, which is the standard treatment of semiclassical laser theory [72,79], to eliminate the two-level atoms in the two cavities. In principle, many phase-space representations (e.g., P presentation, Wigner representation, positive P presentation, etc.) can be used, but in the following we will use Glauber-Sudarshan P presentation [80,81], which is the representation used in laser theory, to achieve our aim. In this formalism, the reduced density matrix $\hat{\rho}$ is represented with a diagonal representation in terms of the coherent states of the photon and phonon, i.e.,

$$\hat{\rho} = \int d^2\alpha_1 d^2\alpha_2 d^2\beta|\alpha_1, \alpha_2, \beta\rangle\langle\alpha_1, \alpha_2, \beta|\hat{\boldsymbol{\rho}}(\alpha_1, \alpha_2, \beta),$$

where $\hat{\boldsymbol{\rho}}$, which is equivalent to the density operator $\hat{\rho}$, is a density operator for the atoms and a quasiprobability distribution for the cavities and the mechanical oscillator over the complex phase-space variables $(\alpha_1, \alpha_2, \beta, \alpha_1^*, \alpha_2^*, \beta^*)$. $|\alpha_j\rangle$ $(j = 1, 2)$ and $|\beta\rangle$ are the coherent states of the jth cavity and the mechanical oscillator, respectively. The quasiprobability distribution for the cavities and mechanical oscillator can be obtained by tracing over the atom space, i.e.,

$$P(\alpha_1, \alpha_2, \beta) = {\rm Tr}_{\rm A}[\hat{\boldsymbol{\rho}}],$$

where ${\rm Tr}_{\rm A}$ stands for tracing over the degree of atoms. In P representation, using the operator correspondences

$$\hat{a}_j\hat{\rho} \to \alpha_j\hat{\boldsymbol{\rho}}, \quad \hat{a}_j^\dagger\hat{\rho} \to \left(\alpha_j^* - \frac{\partial}{\partial\alpha_j}\right)\hat{\boldsymbol{\rho}},$$
$$\hat{\rho}\hat{a}_j^\dagger \to \alpha_j^*\hat{\boldsymbol{\rho}}, \quad \hat{\rho}\hat{a}_j \to \left(\alpha_j - \frac{\partial}{\partial\alpha_j^*}\right)\hat{\boldsymbol{\rho}},$$
$$\hat{b}\hat{\rho} \to \beta\hat{\boldsymbol{\rho}}, \quad \hat{b}^\dagger\hat{\rho} \to \left(\beta^* - \frac{\partial}{\partial\beta}\right)\hat{\boldsymbol{\rho}},$$
$$\hat{\rho}\hat{b}^\dagger \to \beta^*\hat{\boldsymbol{\rho}}, \quad \hat{\rho}\hat{b} \to \left(\beta - \frac{\partial}{\partial\beta^*}\right)\hat{\boldsymbol{\rho}},$$

with $j = 1, 2$, the master equation Eq. (A2) can lead to an equivalent equation in phase space for $\hat{\boldsymbol{\rho}}$, i.e.,

$$\frac{\partial}{\partial t}\hat{\boldsymbol{\rho}} = L_1\hat{\boldsymbol{\rho}} + L_2\hat{\boldsymbol{\rho}} + L_3\hat{\boldsymbol{\rho}}. \quad \text{(A3)}$$

The formulas of L_1, L_2, and L_3 are

$$L_1\hat{\boldsymbol{\rho}} = \mathcal{L}_1\hat{\boldsymbol{\rho}} + \mathcal{L}_2\hat{\boldsymbol{\rho}} + \sum_{j=1}^{2}\sum_{\mu=1}^{N} g_j[\alpha_j^*\hat{\sigma}_{j,\mu}^- - \alpha_j\hat{\sigma}_{j,\mu}^+, \hat{\boldsymbol{\rho}}],$$

$$L_2\hat{\boldsymbol{\rho}} = -\sum_{j=1}^{2}\sum_{\mu=1}^{N} g_j\left[\frac{\partial}{\partial\alpha_j}(\hat{\sigma}_{j,\mu}^- - \langle\hat{\sigma}_{j,\mu}^-\rangle)\hat{\boldsymbol{\rho}} + \frac{\partial}{\partial\alpha_j^*}\hat{\boldsymbol{\rho}}(\hat{\sigma}_{j,\mu}^+ - \langle\hat{\sigma}_{j,\mu}^+\rangle)\right],$$

$$\begin{aligned} L_3\hat{\boldsymbol{\rho}} = {} & \sum_{j=1}^{2}\left[\frac{\partial}{\partial\alpha_j}\left(\kappa\alpha_j - g_j\sum_{\mu=1}^{N}\langle\hat{\sigma}_{j,\mu}^-\rangle\right) + \frac{\partial}{\partial\alpha_j^*}\left(\kappa\alpha_j^* - g_j\sum_{\mu=1}^{N}\langle\hat{\sigma}_{j,\mu}^+\rangle\right)\right]\hat{\boldsymbol{\rho}} + iJ\sum_{j=1}^{2}\left(\frac{\partial}{\partial\alpha_j}\alpha_{3-j} - \frac{\partial}{\partial\alpha_j^*}\alpha_{3-j}^*\right)\hat{\boldsymbol{\rho}} \\ & + i\omega_m\left(\frac{\partial}{\partial\beta}\beta - \frac{\partial}{\partial\beta^*}\beta^*\right)\hat{\boldsymbol{\rho}} + \frac{\gamma_m}{2}\left(\frac{\partial}{\partial\beta}\beta + \frac{\partial}{\partial\beta^*}\beta^*\right)\hat{\boldsymbol{\rho}} + \gamma_m\bar{N}_m\frac{\partial^2}{\partial\beta\partial\beta^*}\hat{\boldsymbol{\rho}} \\ & + i\frac{g_m}{\sqrt{2}}\left[\left(\frac{\partial}{\partial\beta^*} - \frac{\partial}{\partial\beta}\right)\alpha_2\alpha_2^* + \left(\frac{\partial}{\partial\alpha_2^*}\alpha_2^* - \frac{\partial}{\partial\alpha_2}\alpha_2\right)(\beta + \beta^*) + \frac{\partial^2}{\partial\alpha_2\partial\beta}\alpha_2 - \frac{\partial^2}{\partial\alpha_2^*\partial\beta^*}\alpha_2^*\right]\hat{\boldsymbol{\rho}}. \end{aligned}$$

The first term $L_1\hat{\boldsymbol{\rho}}$ is the relevant equation of the atoms and the second term is due to the coupling between the cavities and the atoms. The last term $L_3\hat{\boldsymbol{\rho}}$ represents the free dynamics of the double-cavity optomechanical system. Under the condition $\gamma_1, \gamma_2 \gg \omega_m, \kappa, \gamma_m, g_m$, the atoms can adiabatically follow the dynamics of the optomechanical system and stay in the stationary atomic state $\hat{\rho}_s^A$ which can be derived by using $L_1\hat{\rho}_s^A = 0$. It should be noted that the average values of the ladder operators in L_2 and L_3 are calculated by using $\hat{\rho}_s^A$, i.e., $\langle\hat{\sigma}_{j,\mu}^{\pm}\rangle = \mathrm{Tr}_A[\hat{\sigma}_{j,\mu}^{\pm}\hat{\rho}_s^A]$. Based on this, we can define a projection operator

$$\mathcal{P}\hat{\boldsymbol{\rho}} = P(\boldsymbol{\xi})\hat{\rho}_s^A,$$

where the function $P(\boldsymbol{\xi}) = \mathrm{Tr}_A[\hat{\boldsymbol{\rho}}]$ is the quasiprobability distribution for the cavities and the mechanical oscillator and $\boldsymbol{\xi}$ is the column vector formed from the three pairs of complex variables, i.e., $\alpha_1, \alpha_2, \beta, \alpha_1^*, \alpha_2^*, \beta^*$. It can be easily shown that the projection operator satisfies

$$\mathcal{P}L_1 = L_1\mathcal{P} = 0, \quad \mathcal{P}L_2\mathcal{P} = 0, \quad \mathcal{P}L_3 = L_3\mathcal{P}.$$

Based on the above relation and by using the adiabatic elimination technique [82], the Fokker-Plank (FP) equation for $P(\boldsymbol{\xi})$ can be written as

$$\frac{\partial}{\partial t}P = \left(-\sum_{j=1}^{6}\frac{\partial}{\partial\xi_j}A_j(\boldsymbol{\xi}) + \frac{1}{2}\sum_{i,j}\frac{\partial^2}{\partial\xi_i\partial\xi_j}D_{ij}(\boldsymbol{\xi})\right)P. \tag{A4}$$

The first term in the parentheses is the drift term which determines the deterministic dynamics of the COM and the second term is the diffusion term which is responsible for the noises introduced by the atoms, reservoirs, and optomechanical coupling. The drift vector $\boldsymbol{A}$ is

$$\boldsymbol{A} = \begin{pmatrix} \left(-\kappa + \frac{g_0}{1+\frac{|\alpha_1|^2}{n_1}}\right)\alpha_1 - iJ\alpha_2 \\ \left(-\kappa + \frac{g_0}{1+\frac{|\alpha_1|^2}{n_1}}\right)\alpha_1^* + iJ\alpha_2^* \\ -\left(\kappa + \frac{f_0}{1+\frac{|\alpha_2|^2}{n_2}}\right)\alpha_2 - iJ\alpha_1 + i\frac{g_m}{\sqrt{2}}\alpha_2(\beta + \beta^*) \\ -\left(\kappa + \frac{f_0}{1+\frac{|\alpha_2|^2}{n_2}}\right)\alpha_2^* + iJ\alpha_1^* - i\frac{g_m}{\sqrt{2}}\alpha_2^*(\beta + \beta^*) \\ -i\omega_m\beta + i\frac{g_m}{\sqrt{2}}|\alpha_2|^2 - \frac{\gamma_m}{2}\beta \\ i\omega_m\beta^* - i\frac{g_m}{\sqrt{2}}|\alpha_2|^2 - \frac{\gamma_m}{2}\beta^* \end{pmatrix}.$$

As we only consider the classical dynamics of the system in this paper and the diffusion matrix has no relation with the classical dynamical equations of the system, we do not give the formula of the diffusion matrix here. The gain and loss coefficients are

$$g_0 = \frac{2Ng_1^2}{\gamma_1(2\bar{N}_1 + 1)^2}, \quad f_0 = \frac{2Ng_2^2}{\gamma_2(2\bar{N}_2 + 1)^2},$$

and the gain and loss saturations are

$$n_1 = \frac{\gamma_1^2(2\bar{N}_1 + 1)^2}{8g_1^2}, \quad n_2 = \frac{\gamma_2^2(2\bar{N}_2 + 1)^2}{8g_2^2},$$

respectively. In order to simplify our model further, we assume $n_1 = n_2 = n_0$. In this case, we have $g_0/f_0 = \gamma_1/\gamma_2$, which means that we can turn the ratio between gain and loss coefficients by adjusting the relaxation rates of the gain and loss medium. From the equations of the gain (loss) coefficients and saturations, we can find that the gain and loss coefficients are proportional to the number of the atoms in the cavities of which the gain and loss saturations are independent. This means that we can turn the gain (loss) coefficients and saturations independently by adjusting N and γ_j $(j = 1, 2)$. In this paper, we only consider the classical dynamics of the non-Hermitian COM and neglect the influence of the noises. The classical dynamical equations of the non-Hermitian COM can be derived from the drift term of the FP equation Eq. (A4), i.e., $\langle \dot{\xi}_j \rangle_P = \langle A_j(\boldsymbol{\xi}) \rangle_P$ where the expectation values $\langle \cdot \rangle_P$ are defined by integrals over $P(\boldsymbol{\xi}, t)$ [83]. So the classical dynamical equations of the non-Hermitian COM can be described as

$$\begin{aligned}
\dot{\alpha}_1 &= -\kappa\alpha_1 + \frac{g_0}{1 + \frac{|\alpha_1|^2}{n_0}}\alpha_1 - iJ\alpha_2, \\
\dot{\alpha}_2 &= -\kappa\alpha_2 - \frac{f_0}{1 + \frac{|\alpha_2|^2}{n_0}}\alpha_2 - iJ\alpha_1 + ig_m\alpha_2 x, \\
\ddot{x} &= -\omega_m^2 x + g_m\omega_m|\alpha_2|^2 - \gamma_m\dot{x},
\end{aligned} \tag{A5}$$

where we have changed the equation of β into the equation of $x = (\beta + \beta^*)/\sqrt{2}$. The above equation Eq. (A5) is Eq. (1) in the main text.

[1] C. M. Bender and S. Boettcher, Phys. Rev. Lett. **80**, 5243 (1998).
[2] S. K. Özdemir, S. Rotter, F. Nori, and L. Yang, Nat. Mater. **18**, 783 (2019).
[3] M. Miri and A. Alù, Science **363**, eaar7709 (2019).
[4] Y. Ashida, Z. P. Gong, and M. Ueda, Adv. Phys. **69**, 3 (2020).
[5] T. E. Lee, Phys. Rev. Lett. **116**, 133903 (2016).
[6] L. Jin, Phys. Rev. A **96**, 032103 (2017).
[7] C. H. Lee, L. H. Li, and J. B. Gong, Phys. Rev. Lett. **123**, 016805 (2019).
[8] L. Jin and Z. Song, Phys. Rev. B **99**, 081103(R) (2019).
[9] Z. P. Gong, Y. Ashida, K. Kawabata, K. Takasan, S. Higashikawa, and M. Ueda, Phys. Rev. X **8**, 031079 (2018).
[10] F. K. Kunst, E. Edvardsson, J. C. Budich, and E. J. Bergholtz, Phys. Rev. Lett. **121**, 026808 (2018).
[11] S. Y. Yao and Z. Wang, Phys. Rev. Lett. **121**, 086803 (2018).
[12] H. C. Wu, L. Jin, and Z. Song, Phys. Rev. B **100**, 155117 (2019).
[13] S. Lin, L. Jin, and Z. Song, Phys. Rev. B **99**, 165148 (2019).
[14] K. L. Zhang, H. C. Wu, L. Jin, and Z. Song, Phys. Rev. B **100**, 045141 (2019).
[15] S. Y. Yao, F. Song, and Z. Wang, Phys. Rev. Lett. **121**, 136802 (2018).
[16] H. T. Shen, B. Zhen, and L. Fu, Phys. Rev. Lett. **120**, 146402 (2018).
[17] L. H. Li, C. H. Lee, and J. B. Gong, Phys. Rev. B **100**, 075403 (2019).
[18] K. G. Makris, R. El-Ganainy, D. N. Christodoulides, and Z. H. Musslimani, Phys. Rev. Lett. **100**, 103904 (2008).
[19] Z. H. Musslimani, K. G. Makris, R. El-Ganainy, and D. N. Christodoulides, Phys. Rev. Lett. **100**, 030402 (2008).
[20] C. E. Rüter, K. G. Makris, R. El-Ganainy, D. N. Christodoulides, M. Segev, and D. Kip, Nat. Phys. **6**, 192 (2010).
[21] A. Regensburger, C. Bersch, M. A. Miri, G. Onishchukov, D. N. Christodoulides, and U. Peschel, Nature (London) **488**, 167 (2012).
[22] B. Peng, S. K. Ozdemir, F. C. Lei, F. Monifi, M. Gianfreda, G. L. Long, S. H. Fan, F. Nori, C. M. Bender, and L. Yang, Nat. Phys. **10**, 394 (2014).
[23] C. M. Bender, M. Gianfreda, S. K. Özdemir, B. Peng, and L. Yang, Phys. Rev. A **88**, 062111 (2013).
[24] Z. P. Liu, J. Zhang, S. K. Özdemir, B. Peng, H. Jing, X. Y. Lü, C. W. Li, L. Yang, F. Nori, and Y. X. Liu, Phys. Rev. Lett. **117**, 110802 (2016).
[25] I. I. Arkhipov, A. Miranowicz, F. Minganti, and F. Nori, Phys. Rev. A **101**, 013812 (2020).
[26] X. B. Luo, J. H. Huang, H. H. Zhong, X. Z. Qin, Q. T. Xie, Y. S. Kivshar, and C. H. Lee, Phys. Rev. Lett. **110**, 243902 (2013).
[27] B. Y. Yang, X. B. Luo, Q. L. Hu, and X. G. Yu, Phys. Rev. A **94**, 043828 (2016).
[28] J. Zhang, B. Peng, S. K. Özdemir, Y. X. Liu, H. Jing, X. Y. Lü, Y. L. Liu, L. Yang, and F. Nori, Phys. Rev. B **92**, 115407 (2015).
[29] X. F. Zhu, H. Ramezani, C. Z. Shi, J. Zhu, and X. Zhang, Phys. Rev. X **4**, 031042 (2014).
[30] R. Fleury, D. Sounas, and A. Alù, Nat. Commun. **6**, 5905 (2015).
[31] K. V. Kepesidis, T. J. Milburn, J. L. Huber, K. G. Makris, S. Rotter, and P. Rabl, New J. Phys. **18**, 095003 (2016).
[32] H. Ramezani, J. Schindler, F. M. Ellis, U. Günther, and T. Kottos, Phys. Rev. A **85**, 062122 (2012).
[33] Z. Lin, J. Schindler, F. M. Ellis, and T. Kottos, Phys. Rev. A **85**, 050101(R) (2012).
[34] J. Schindler, A. Li, M. C. Zheng, F. M. Ellis, and T. Kottos, Phys. Rev. A **84**, 040101(R) (2011).
[35] F. Quijandría, U. Naether, S. K. Özdemir, F. Nori, and D. Zueco, Phys. Rev. A **97**, 053846 (2018).
[36] X. B. Luo, B. Y. Yang, X. F. Zhang, L. Li, and X. G. Yu, Phys. Rev. A **95**, 052128 (2017).
[37] H. Benisty *et al.*, Opt. Express **19**, 18004 (2011).
[38] M. Kang, F. Liu, and J. Li, Phys. Rev. A **87**, 053824 (2013).

[39] J. Doppler, A. A. Mailybaev, J. Böhm, U. Kuhl, A. Girschik, F. Libisch, T. J. Milburn, P. Rabl, N. Moiseyev, and S. Rotter, Nature (London) **537**, 76 (2016).

[40] A. U. Hassan, G. L. Galmiche, G. Harari, P. LiKamWa, M. Khajavikhan, M. Segev, and D. N. Christodoulides, Phys. Rev. A **96**, 052129 (2017).

[41] M. Brandstetter, M. Liertzerm, C. Deutsch, P. Klang, J. Schoberl, H. E. Tureci, G. Strasser, K. Unterrainer, and S. Rotter, Nat. Commun. **5**, 4034 (2014).

[42] B. Peng, S. K. Özdemir, S. Rotter, H. Yilmaz, M. Liertzer, F. Moninfi, C. M. Bender, F. Nori, and L. Yang, Science **346**, 328 (2014).

[43] H. Hodaei, A. U. Hassan, S. Wittek, H. Garcia-Gracia, R. El-Ganainy, D. N. Christodoulides, and M. Khajavikhan, Nature (London) **548**, 187 (2017).

[44] W. Chen, S. K. Özdemir, G. Zhao, J. Wiersig, and L. Yang, Nature (London) **548**, 192 (2017).

[45] V. M. Martinez Alvarez, J. E. Barrios Vargas, and L. E. F. Foa Torres, Phys. Rev. B **97**, 121401(R) (2018).

[46] C. H. Lee and R. Thomale, Phys. Rev. B **99**, 201103(R) (2019).

[47] L. Feng, Z. J. Wong, R. M. Ma, Y. Wang, and X. Zhang, Science **346**, 972 (2014).

[48] H. Hodaei, M. A. Miri, M. Heinrich, D. N. Christodoulides, and M. Khajavikhan, Science **346**, 975 (2014).

[49] Z. Lin, H. Ramezani, T. Eichelkraut, T. Kottos, H. Cao, and D. N. Christodoulides, Phys. Rev. Lett. **106**, 213901 (2011).

[50] L. Feng, Y. L. Xu, W. S. Fegadolli, M. H. Lu, J. E. B. Oliveira, V. R. Almeida, Y. F. Chen, and A. Scherer, Nat. Mater. **12**, 108 (2013).

[51] X. Yin and X. Zhang, Nat. Mater. **12**, 175 (2013).

[52] S. Longhi, Phys. Rev. A **82**, 031801(R) (2010).

[53] Y. D. Chong, L. Ge, and A. D. Stone, Phys. Rev. Lett. **106**, 093902 (2011).

[54] Y. Sun, W. Tan, H. Q. Li, J. S. Li, and H. Chen, Phys. Rev. Lett. **112**, 143903 (2014).

[55] W. L. Li, Y. F. Jiang, C. Li, and H. S. Song, Sci. Rep. **6**, 31095 (2016).

[56] H. Jing, S. K. Özdemir, X. Y. Lü, J. Zhang, L. Yang, and F. Nori, Phys. Rev. Lett. **113**, 053604 (2014).

[57] X. Y. Lü, H. Jing, J. Y. Ma, and Y. Wu, Phys. Rev. Lett. **114**, 253601 (2015).

[58] D. W. Schönleber, A. Eisfeld, and R. El-Ganainy, New J. Phys. **18**, 045014 (2016).

[59] S. Vashahri-Ghamsari, B. He, and M. Xiao, Phys. Rev. A **96**, 033806 (2017).

[60] G. S. Agarwal and K. Qu, Phys. Rev. A **85**, 031802(R) (2012).

[61] A. U. Hassan, H. Hodaei, M. A. Miri, M. Khajavikhan, and D. N. Christodoulides, Phys. Rev. A **92**, 063807 (2015).

[62] B. He, L. Yang, X. Jiang, and M. Xiao, Phys. Rev. Lett. **120**, 203904 (2018).

[63] D. R. Barton, H. Alaeian, M. Lawrence, and J. Dionne, Phys. Rev. B **97**, 045432 (2018).

[64] S. Sunada, Phys. Rev. A **97**, 043804 (2018).

[65] M. H. Teimourpour, A. Rahman, K. Srinivasan, and R. El-Ganainy, Phys. Rev. Appl. **7**, 014015 (2017).

[66] Y. F. Xie, Z. Cao, B. He, and Q. Lin, Opt. Express **28**, 22580 (2020).

[67] B. He, L. Yang, and M. Xiao, Phys. Rev. A **94**, 031802(R) (2016).

[68] J. Zhang, B. Peng, S. L. Özdemir, K. Pichler, D. O. Krimer, G. P. Zhao, F. Nori, Y. X. Liu, S. Rotter, and L. Yang, Nat. Photon. **12**, 479 (2018).

[69] I. I. Arkhipov, A. Miranowicz, O. Di Stefano, R. Stassi, S. Savasta, F. Nori, and S. K. Özdemir, Phys. Rev. A **99**, 053806 (2019).

[70] L. Chang, X. S. Jiang, S. Y. Hua, C. Yang, J. M. Wen, L. Jiang, G. Y. Li, G. Z. Wang, and M. Xiao, Nat. Photon. **8**, 524 (2014).

[71] Z. Cao, Y. F. Xie, B. He, and Q. Lin, New J. Phys. **23**, 023010 (2021).

[72] C. W. Gardiner and P. Zoller, *Quantum Noise*, 2nd ed. (Springer-Verlag, Berlin, 2000).

[73] V. S. Anishchenko, T. E. Vadivasova, and G. I. Strelkova, *Deterministic Nonlinear Systems: A Short Course*, 1st ed. (Springer-Verlag, Berlin, 2014).

[74] A. Cerjan, Y. D. Chong, L. Ge, and A. D. Stone, Opt. Express **20**, 474 (2011).

[75] F. Marquardt, J. G. E. Harris, and S. M. Girvin, Phys. Rev. Lett. **96**, 103901 (2006).

[76] E. Verhagen, S. Deleglise, S. Weis, A. Schliesser, and T. J. Kippenberg, Nature (London) **482**, 63 (2012).

[77] I. S. Grudinin, H. Lee, O. Painter, and K. J. Vahala, Phys. Rev. Lett. **104**, 083901 (2010).

[78] R. J. Glauber, *Quantum Theory of Optical Coherence* (Wiley, New York, 2007).

[79] F. Haake and M. Lewenstein, Phys. Rev. A **27**, 1013 (1983).

[80] R. J. Glauber, Phys. Rev. **131**, 2766 (1963).

[81] E. C. G. Sudarshan, Phys. Rev. Lett. **10**, 277 (1963).

[82] C. W. Gardiner, *Stochastic Methods*, 4th ed. (Springer-Verlag, Berlin, 2009).

[83] D. F. Walls and G. J. Milburn, *Quantum Optics* (Springer-Verlag, Berlin, 1994).